

# Water film thickness-dependent conformation and diffusion of single-strand DNA on poly(ethylene glycol)-silane surface

Jae Hyun Park and N. R. Aluru<sup>a)</sup>

Department of Mechanical Science and Engineering, Beckman Institute for Advanced Science and Technology, University of Illinois at Urbana-Champaign, Urbana, Illinois 61801, USA

(Received 26 December 2009; accepted 24 February 2010; published online 24 March 2010)

In this paper, we investigate, using molecular dynamics simulations, the conformation and diffusion of longer and shorter single-strand DNA (ssDNA) as a function of water film thickness. While the conformation of the shorter ssDNA is significantly affected and the diffusion is suppressed with reduction in water film thickness, the conformation and diffusion of the longer DNA is not influenced. We explain our observations by considering the competition between stacking interaction of bases and solvation tendency of ssDNA. This paper suggests an approach to control the surface motion of ssDNA in nanoscale water films using film thickness. © 2010 American Institute of Physics. [doi:10.1063/1.3366725]

DNA separation is an essential technique for gene sequencing and DNA fingerprinting. The development of accurate and versatile DNA separation technique is currently a significant issue in nanobiotechnology.<sup>1</sup> Recently, Pernodet *et al.*<sup>2</sup> reported separation of DNA chains on a surface without any topological restrictions or any solution sieving media. This can be a significant benefit over conventional separation methods. However, a detailed physical understanding of surface transport of DNA is currently not available.<sup>3</sup> For example, it is commonly known that the diffusion coefficient of DNA decreases with increase in DNA size in free solution<sup>4</sup> and under two-dimensional confinement.<sup>5</sup> However, a recent experimental study on electrophoresis of DNA on an atomic force microscopy surface showed the faster movement of longer DNA in a thin pure water film.<sup>6</sup> According to the Nernst–Einstein relation between mobility and diffusion, this implies that the longer DNA has higher diffusion than the shorter DNA.

To understand the reasons behind the ambiguities in the physics of surface transport of DNA, in this paper, we investigate, using extensive molecular dynamics (MD) simulations, the diffusion of DNA in nanometer-thick water films by considering DNA of various sizes. As shown in the schematic in Fig. 1(a), a single-strand DNA (ssDNA) was solvated in a pure water film on a solid surface. Following the experiment,<sup>6</sup> the surface was made by grafting the poly(ethylene glycol)-silanes (PEG-silanes) on a solid substrate. The size of the surface is  $20 \times 20 \text{ nm}^2$  and it consists of 1600 PEG-silane molecules. The PEG-silane has 32 atoms and it is attached to the substrate atom [see Fig. 1(b)]. The initial configuration and the atomic partial charges of PEG-silane molecule were obtained from PRODRG (Ref. 7) using GROMOS forcefield and charge. The substrate atoms were assumed frozen and their atomic charges were adjusted to make the entire system neutral. We considered two small ssDNAs fragments with 6 and 12 bases. Although recent DNA sequencing technologies utilize tens of millions of small DNA fragments,<sup>8</sup> efficient separation of such small fragments is still challenging.<sup>9</sup> The longer 12-base ssDNA

of 5′–CGCGAATTCGCG–3′ was prepared by unzipping the well-known Dickerson’s B-DNA dodecamer (double stranded),<sup>10</sup> while the shorter 6-base ssDNA of 5′–CGCGAG–3′ was made by repeating the initial five bases of the 12 base DNA and ending with 3′–G. Two water films were considered with  $L=2.3 \text{ nm}$  [thick film, see Fig. 1(c)] and  $L=1.4 \text{ nm}$  [thin film, see Fig. 1(d)], where  $L$  is the film thickness defined as the distance between the crossing point of PEG and water and the point where the water density value is half the bulk density in water film [see Figs. 1(c) and 1(d)]. All the simulations in the present study were performed using GROMACS 4.0.4 (Ref. 11) in an NVT ensemble. The AMBER-99 force field and the atomic partial charges<sup>12</sup> were introduced into GROMACS using the AMBER force field port.<sup>13</sup> Periodic boundary conditions were assigned along  $x$ - and  $y$ -directions. All the simulations were equilibrated for 1.5 ns. The sampling period was 900 ps. Water was modeled by using the TIP3P model.<sup>14</sup> The Noé–Hoover thermostat<sup>15</sup> was used to maintain the system temperature at 300 K. The equation of motion was integrated by using the leapfrog algorithm with a time step of 2.0 fs.

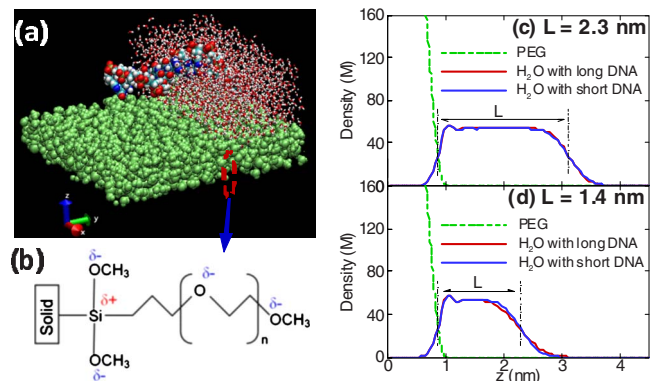


FIG. 1. (Color online) (a) Molecular visualization of ssDNA in water film on PEG-silane grafted surface. The surface lies along the  $xy$ -plane. The snapshot was rendered with (Visual Molecular Dynamics, Ref. 23). The red ball is the oxygen atom, white is the hydrogen atom, blue is the nitrogen atom, cyan is the carbon atom, and tan is the phosphorus atom; (b) Structure of PEG-silane molecule; (c) Density plots of water and PEG for the thick water film; (d) Density plots of water and PEG for the thin water film. For the examples considered here, water density was not significantly influenced by the DNA type.

<sup>a)</sup> Author to whom correspondence should be addressed. Electronic mail: aluru@illinois.edu.

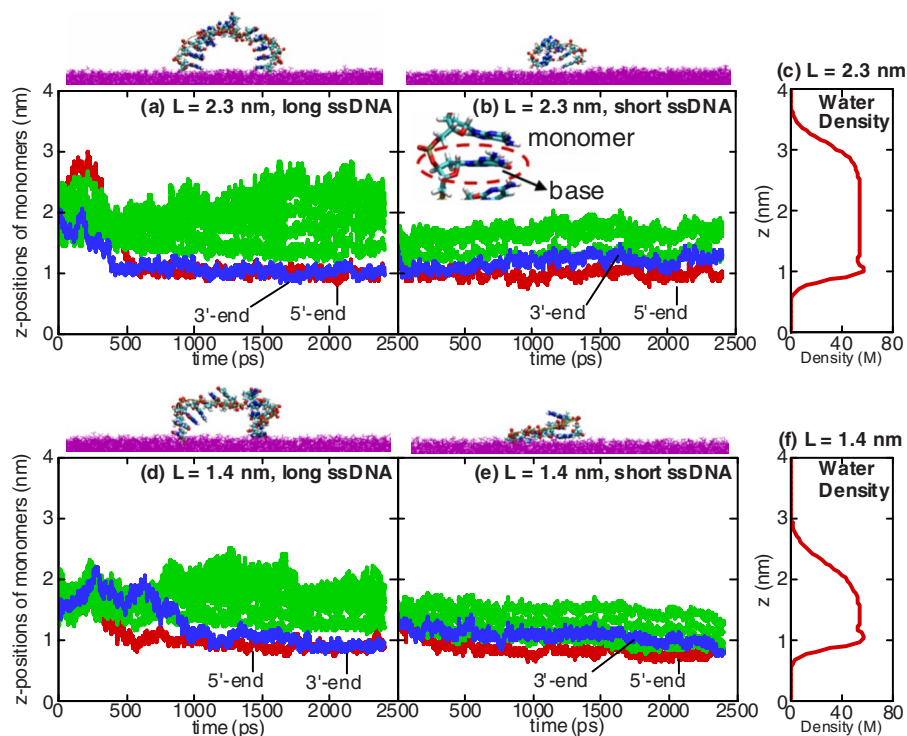


FIG. 2. (Color online) Temporal variation of the  $z$ -position of the monomers in ssDNA and the typical DNA conformation in equilibrium state: (a)  $L = 2.3$  nm, long 12-base ssDNA. Red and blue lines represent the 5' and 3'-end monomers, respectively. The green lines are the middle monomers in the DNA; (b)  $L = 2.3$  nm, short 6-base ssDNA; (c) water density of thick film; (d)  $L = 1.4$  nm, long 12-base ssDNA; (e)  $L = 1.4$  nm, short 6-base ssDNA; (f) water density of thin film.

In Fig. 2, we show the temporal variation of the  $z$ -position of each monomer of ssDNA for different film thicknesses and DNA sizes. The typical conformations in equilibrium state were also visualized. In the present study, the monomer of DNA was defined as the combined structure of a base and the linked nucleotide backbone [see the inset in Fig. 2(b)]. The equilibrium state of a biopolymer (e.g., ssDNA) on surface can be confirmed by investigating the motion of each monomer as each monomer may have considerable motion even though the center of mass motion of DNA is in steady-state (cf. similar to equilibrium). As shown in Fig. 2, all the ssDNAs were equilibrated after  $t > 1.5$  ns. The discussion below on Fig. 2 is for the equilibrated conformations unless specified otherwise. For the long ssDNA in the thick water film with  $L = 2.3$  nm, both the 5'- and 3'-end monomers were attached on the surface while the other monomers were detached from the surface [see Fig. 2(a)]. The conformation of long ssDNA in thick water film did not vary as  $L$  was reduced to 1.4 nm [see Fig. 2(c)]. In contrast, in the case of short ssDNA, a considerable difference was observed. For the short 6-base ssDNA in the thick water film, only the end monomers were attached on the surface while the other monomers were detached from the surface [see Fig. 2(b)], which is similar to the conformation of long ssDNA. However, in the thin water film, all the monomers were attached on the surface [see Fig. 2(e)].

For the motion of ssDNA on the surface considered here, there are two competing factors. The first is the structural robustness. The bases in ssDNA can be stacked on top of each other. The parallel interaction between stacked bases stabilizes the DNA structure.<sup>16</sup> Using the free energies of stacking for base pairs with AMBER force field,<sup>17</sup> the total free energy reduction by stacking was computed as  $-60.76$  kcal/mol for the longer ssDNA and  $-30.34$  kcal/mol for the shorter ssDNA. The longer ssDNA has more number of bases in stacking interaction and it makes the ssDNA structure more robust. However, the shorter ssDNA has less num-

ber of bases and it makes the structure less robust. The second competing factor is the solvation tendency of DNA. DNA usually has strong tendency to be solvated in the water, expressed by the low solvation free energy. The solvation free energy of the biopolymer (e.g., ssDNA) can be estimated using the generalized Born approximation.<sup>18</sup> From the generalized Born approximation, employing the parameters optimized for AMBER DNA force field,<sup>19</sup> the solvation free energies in bulk water were estimated as  $-54.2$  kJ/mol for the longer 12-base ssDNA and  $-28.2$  kJ/mol for the shorter 6-base ssDNA. Such low solvation free energy will become a driving force for DNA to locate in the water-rich region, which is near the water-surface interface, rather than the air-water interface. Since ssDNA prefers to stay in the water-rich region, with decrease in  $L$ , they approach the PEG-silane surface. Thus, the shorter ssDNA was deformed due to the weak structural robustness, which was not strong enough to overcome DNA-surface interaction. However, the longer ssDNA was not deformed due to the strong structural robustness, which was enough to maintain the structure overcoming the DNA-surface interaction.

The conformational differences between the shorter and the longer ssDNA can lead to different transport properties of ssDNA (e.g., diffusion). The lateral diffusion coefficient can be computed from the mean-squared displacement plot as  $D = \lim_{t \rightarrow \infty} \langle |\mathbf{R}_{\text{CM}}(t) - \mathbf{R}_{\text{CM}}(0)|^2 \rangle / 4t$ , where  $\mathbf{R}_{\text{CM}}$  is the  $(x, y)$ -position of the center-of-mass of ssDNA. Throughout this paper, diffusion coefficient refers to the lateral diffusion coefficient unless specified, otherwise. Table I compares the

TABLE I. Diffusion coefficient of ssDNA ( $\times 10^{-10}$  m<sup>2</sup>/s).

$L$ (nm)	Long ssDNA	Short ssDNA
2.3	1.76 ( $\pm 0.17$ )	3.23 ( $\pm 0.56$ )
1.4	1.82 ( $\pm 0.48$ )	0.53 ( $\pm 0.10$ )

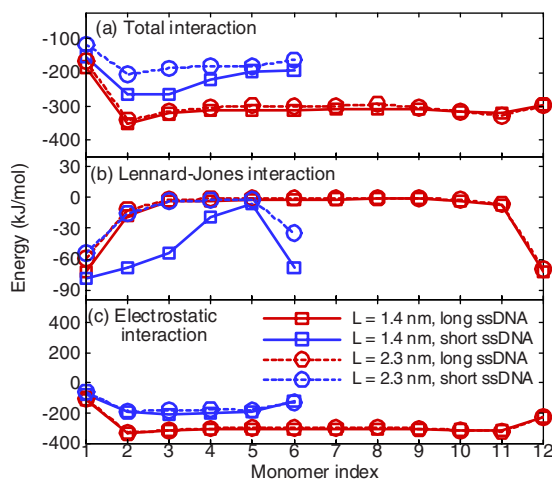


FIG. 3. (Color online) Comparison of the interaction energy between monomer in ssDNA and surface: (a) total interaction; (b) LJ interaction; (c) electrostatic interaction.  $x$ -axis is the index of the monomer in ssDNA.

diffusion coefficients for the longer and shorter ssDNA in thin and thick water films. We note from the results in the table that the diffusion coefficient of the shorter 6-base ssDNA is significantly reduced in the thin water film while the diffusion coefficient of the longer 12-base ssDNA was not influenced by the change in  $L$  considering the error level. This trend can be explained from the trend in molecular conformation shown in Fig. 2. The diffusion behavior can be further probed by examining the interaction energy between ssDNA and the surface. For the cases considered here, a strong water layering was not observed, so the anomalous behavior of water on surfaces is not significant.<sup>20</sup> Figure 3(a) shows the total interaction energy between monomer of ssDNA and surface. The total interaction energy was computed by summing all the pairwise Lennard-Jones (LJ) and electrostatic interaction energies between atoms in DNA and those in the PEG-silane surface. For the longer ssDNA, the interaction energy did not vary significantly with  $L$ , while for the shorter ssDNA, the interaction energy decreases with decrease in  $L$ . The stronger interaction of DNA with the surface lowers the diffusion coefficient.

Next, we compare the diffusion coefficients of the long and short ssDNAs in  $L=2.3$  and  $1.4$  nm (see Table I). In bulk, the shorter biopolymer (e.g., ssDNA) typically moves faster compared to the longer one.<sup>4</sup> The diffusion coefficient of the longer 12-base ssDNA is  $2.68 (\pm 0.34) \times 10^{-10}$  m<sup>2</sup>/s and the diffusion coefficient of the shorter 6-base ssDNA is  $4.81 (\pm 0.43) \times 10^{-10}$  m<sup>2</sup>/s in bulk solution. This trend was also observed in the thick water film. However, in the thin water film, the trend is opposite, i.e., the longer ssDNA moves faster compared to the shorter one. This is because of the considerable immobilization of the shorter ssDNA by the water film-thickness resulting in ssDNA deformation and a stronger short-range LJ interaction between DNA and surface. Figure 3 shows that in the thin water film, both the total and the electrostatic interaction energies were lower for the longer ssDNA compared to the shorter ssDNA due to the higher net charge on the longer ssDNA [see Figs. 3(a) and 3(c)]. However, for the short-range LJ interaction energy, the

shorter ssDNA has the lower value [see Fig. 3(b)]. The deformation of the shorter ssDNA on the surface causes the increase in the short-range LJ interaction,<sup>21</sup> which results in lower diffusion of the shorter ssDNA.

In summary, the conformation and diffusion of ssDNA can depend on the thickness of the water film on a surface. In particular, the conformation and diffusion of the short ssDNA was affected by the reduction of water film thickness due to the competition between structural robustness and solvation tendency. In the thin water film, the shorter ssDNA moved slower compared to the longer ssDNA due to the stronger short-range LJ interaction. The fundamental understanding developed here for motion of ssDNA on a solid surface would be helpful in enabling further advances in surface-based DNA separations and protein fingerprinting.<sup>22</sup>

This research was supported by NSF under Grant Nos. 0120978, 0328162, 0810294, 0852657, and 0915718, and by NIH under Grant No. PHS 2 PN2 EY016570B.

- <sup>1</sup>F. Wan, J. Zhang, and B. Chu, in *Advances in Chromatography*, edited by E. Grushka and N. Grinberg (CRC, Boca Raton, FL, 2009), Vol. 47, Chap. 3, pp. 59–125; Y.-S. Seo, H. Luo, V. A. Samuilov, M. H. Rafailovich, J. Sokolov, D. Gersappe, and B. Chu, *Nano Lett.* **4**, 659 (2004).
- <sup>2</sup>N. Pernodet, V. A. Samuilov, K. Shin, J. Sokolov, M. H. Rafailovich, D. Gersappe, and B. Chu, *Phys. Rev. Lett.* **85**, 5651 (2000).
- <sup>3</sup>G. W. Slater, C. Holm, M. V. Chubynsky, H. W. de Haan, A. Dube, K. Grass, O. A. Hickey, C. Kingsbury, D. Sean, T. N. Shendruk, and L. Zhan, *Electrophoresis* **30**, 792 (2009).
- <sup>4</sup>A. E. Nkodo, J. M. Garnier, B. Tinland, H. Ren, C. Desruisseaux, L. C. McCormick, G. Drouin, and G. W. Slater, *Electrophoresis* **22**, 2424 (2001).
- <sup>5</sup>B. Maier and J. O. Rädler, *Phys. Rev. Lett.* **82**, 1911 (1999).
- <sup>6</sup>K. Unal, J. Frommer, and H. K. Wickramasingh, *Appl. Phys. Lett.* **88**, 183105 (2006).
- <sup>7</sup>A. W. Schüttelkopf and D. M. F. van Aalten, *Acta Crystallogr., Sect. D: Biol. Crystallogr.* **60**, 1355 (2004).
- <sup>8</sup>H. Li, J. Ruan, and R. Durbin, *Genome Res.* **18**, 1851 (2008).
- <sup>9</sup>J. Fu, R. B. Schoch, A. L. Stevens, S. R. Tannenbaum, and J. Han, *Nat. Nanotechnol.* **2**, 121 (2007).
- <sup>10</sup>H. R. Drew, R. M. Wing, T. Takano, C. Broka, S. Tanaka, K. Itakura, and R. E. Dickerson, *Proc. Natl. Acad. Sci. U.S.A.* **78**, 2179 (1981).
- <sup>11</sup>D. Van Der Spoel, E. Lindahl, B. Hess, G. Groenhof, A. E. Mark, and H. J. C. Berendsen, *J. Comput. Chem.* **26**, 1701 (2005).
- <sup>12</sup>J. Wang, P. Cieplak, and P. A. Kollman, *J. Comput. Chem.* **21**, 1049 (2000).
- <sup>13</sup>E. J. Sorin and V. S. Pande, *Biophys. J.* **88**, 2472 (2005).
- <sup>14</sup>W. L. Jorgensen, J. Chandrasekhar, J. D. Madura, R. W. Impley, and M. L. Klein, *J. Chem. Phys.* **79**, 926 (1983).
- <sup>15</sup>S. Nosé, *Mol. Phys.* **52**, 255 (1984); W. G. Hoover, *Phys. Rev. A* **31**, 1695 (1985).
- <sup>16</sup>W. Saenger, *Principles of Nucleic Acid Structure* (Springer, New York, 1988), pp. 132–140.
- <sup>17</sup>R. A. Friedman and B. Honig, *Biophys. J.* **69**, 1528 (1995).
- <sup>18</sup>W. C. Still, A. Tempczyk, R. C. Hawley, and T. Hendrickson, *J. Am. Chem. Soc.* **112**, 6127 (1990); D. Bashford and D. A. Case, *Annu. Rev. Phys. Chem.* **51**, 129 (2000).
- <sup>19</sup>B. Jayaram, D. Sprous, and D. L. Beveridge, *J. Phys. Chem. B* **102**, 9571 (1998).
- <sup>20</sup>J. H. Park and N. R. Aluru, *Appl. Phys. Lett.* **93**, 253104 (2008).
- <sup>21</sup>M. C. P. van Eijk, M. A. Cohen Stuart, and G. J. Fleer, *Prog. Colloid Polym. Sci.* **105**, 31 (1997).
- <sup>22</sup>P. Ramasamy, M. R. Elmaghrabi, G. Halada, and M. Rafailovich, MRS Symposia Proceedings No. 1061 (Materials Research Society, Pittsburgh, 2008), p. 1061–MM09–23.
- <sup>23</sup>W. Humphrey, A. Dalke, and K. Schulten, *J. Mol. Graph.* **14**, 33 (1996).